Using multiple trait associations to define hydraulic functional types in plant communities of south-western Australia

Patrick J. Mitchell[1 *], Erik Veneklaas[1] , Hans Lambers[1] and Stephen S. O. Burgess[1]

[1]*School of Plant Biology, University of Western Australia and the Cooperative Research Centre for Plant-Based Management of Dryland Salinity, 35 Stirling Highway, Crawley WA 6009 AUSTRALIA*

* corresponding author: pjm@unimelb.edu.au

ph: +61 3 8344 9304 fax: +61 3 8344 5570

Abstract

Assessing the hydrologic imbalance and associated land degradation issues facing much of southern Australia and other parts of the world requires a better understanding of the defining features of ecosystem water use and the design of sustainable agroecosystems. The water use characteristics of species-rich plant communities in south-western Australia were assessed by grouping species with similar water use strategies into 'hydraulic functional types' (HFTs). HFTs were determined using multiple-trait associations between morphological and physiological traits relating to water transport, water use efficiency and response to water deficit. Sixteen traits were assessed from a subset of 21 species from three plant communities located along a topographically determined soil and water-availability gradient. Multivariate analyses showed that trait variation was least at sites with shallower soils and putatively lower water availability, suggesting a convergence of water use strategies at sites where plants are exposed to large seasonal water deficits. Stem hydraulic parameters, including stem-specific hydraulic conductivity, conduit diameter and maximum percentage embolism, were positively correlated, indicating the generality that larger conduit diameter permits greater hydraulic efficiency and is associated with greater seasonal reductions in hydraulic conductivity in this ecosystem. Wood density was not correlated with these traits, but closely associated with species' ability to withstand more negative water potentials during summer. Long-term integrated water use efficiency was lower in shallow-rooted species that exhibited more negative summer water potentials. Specific leaf area and minimum leaf water potential were correlated with a number of separate traits, and appear to represent key axes of trait variation that describe the water use strategies of different HFTs along the topographic gradient. Five HFTs were classified using a resemblance analysis according to combinations of traits that pertain to different water use strategies among species; year-round active tree,

year-round active shrub, hemiparasite, drought-suppressed broad-leaved shrub and drought-suppressed narrow-leaved shrub.

Keywords: functional traits, specific leaf area, water potential, water use strategy, ecohydrology

Introduction

Transpiration varies both spatially and temporally within plant communities, due to differences in water availability within the soil, atmospheric conditions, and plant form and functioning. In southern Australia, changes to transpiration capacity of landscapes via changes to the vegetation composition and structure that have accompanied land clearing and agricultural practices have had dramatic effects on the hydrologic balance within the landscape. This has caused saline groundwater levels to rise and led to the expansion of dryland salinity (Hatton et al. 2003; Peck and Hatton 2003). Addressing this imbalance requires a better understanding of the relationship between vegetation and landscape hydrology; studying the defining features of native ecosystem water use has the potential to assist with the design of sustainable agroecosystems.

In water-limited Mediterranean-type ecosystems such as south-western Australia, the availability of water is a major factor shaping the structure and composition of plant communities and the diverse array of functional attributes of plants both above- and below-ground. There are a broad suite of traits that influence a plant's ability to respond to variations in water availability including rooting depth and morphology, stomatal response, leaf physiology, leaf phenology and hydraulic architecture. In many cases, associated plant traits cannot be optimised simultaneously owing to underlying biophysical constraints: the

result is trade-offs that may apply across taxa and ecosystems. In relation to plant water use strategies, trade-offs may generally apply to a species' capacity for rapid growth versus drought hardiness. Recent studies that have addressed global-scale trade-offs in key plant traits, support the concept of functional convergence in plant traits associated with carbon and water balance (Enquist 2003; Meinzer 2003; Reich et al. 1997; Westoby et al. 2002). Studies across several different ecosystems and/or biomes have defined trade-offs with respect to leaf carbon economy and leaf structure (Wright et al. 2004), sapwood density and water transport and safety (Hacke et al. 2001; Preston and Ackerly 2003), and allometry and water transport (Enquist and Niklas 2001; Meinzer et al. 2001). Traits that determine water balance are interrelated and combine to determine a particular plant water use strategy that allows species to maximise their fitness within their environment under daily, seasonal, interannual and even interdecadal fluctuations in water availability.

Gauging the whole suite of water use strategies within a species-rich plant community requires a description of the ecosystem in terms of the specific hydrologic function of individual species. Under the plant functional type concept, species sharing similar ecological function are grouped together using context-specific traits, independent of taxonomic groupings (Woodward and Kelly 1997). The appropriate functional traits are used as screening tools in order to filter species according to their function at a scale that is appropriate to the research question (Keddy 1992). On a broad scale, Mediterranean type ecosystems have generally been divided into two functional types, where classifications based primarily on phenology have identified evergreen sclerophylls and drought-semi-deciduous types, or using response characteristics such as to fire and drought, produced two distinct groups of 'seeders' and 'resprouters' (Meentemeyer and Moody 2002; Ackerly 2004). These classifications have little application to Mediterranean-type ecosystems of

southern Australia where very few species exhibit any deciduous habits, and may over-simplify finer-scale distinctions in water use strategies among the species-rich plant communities of this region. Therefore, we have introduced the concept of the 'hydraulic functional type' (HFT) to examine the water use related structure of plant communities, growing along topographically determined gradients in soils and water availability.

The occurrence of multiple HFTs in a plant community can be interpreted as a form of niche partitioning by which co-existence of multiple species is promoted. The ability of species to fill available niches in space and time maximises resource utilisation and promotes ecohydrological equilibrium, i.e. water supply and demand are closely matched (Hatton et al. 1997). In water-limited environments such as south-western Australia, overall vegetation properties such as percentage plant cover are strongly constrained at a regional scale by a limited set of environmental constraints: precipitation, evaporative demand and soil storage capacity (Eagleson 1982; Hatton et al. 1997). However, over smaller spatial scales, where climatic differences do not play a role, shifts in vegetation structure and composition occur along topographically determined gradients and vegetation may differ considerably in community-scale transpiration properties. The species-rich plant communities in south-western Australia are particularly shaped by soil-vegetation associations (Beard 1980), where local scale community composition is largely defined by topographical variation arising from the deeply weathered lateritic profiles (Dirnböck et al. 2002). The species-rich communities located along these topographical gradients are likely to contain differing combinations of HFTs that optimise plant water utilisation and long-term survival at a given site under local conditions. For example, at sites with inherent limitations on plant water availability, unsuitable 'profligate' or summer-active HFTs may be absent from the community, with a trend instead toward conservative HFTs.

We sought to characterise the predominant plant water use strategies and main HFTs present in a subset of species from three native plant communities along a topographical gradient in south-western Australia. We used a 'bottom-up' approach starting with the measurement of relevant morphological and physiological traits to group species with similar trait positioning using multivariate analyses. Using this approach, we addressed the following questions. How do differences in soil water availability arising from differences in landscape position affect the overall variation in trait values (within and between sites) and mix of HFTs along this gradient? What are the most important traits associated with particular HFTs? Among the traits used in this study, what are the key dimensions of trait variation that underpin the positioning of HFTs along the water-availability gradient?

Materials and Methods

Study Site

The study site was located approximately 2 km west of Corrigin, Western Australia, Australia (32º 19' S, 117º 52'E) at the Corrigin Water Reserve. This 1096 ha remnant of native vegetation is typical of the region prior to land-clearing for agriculture, and contains a range of plant communities and over 500 native plant species. These communities are closely associated with a catenary sequence along the landscape, consisting of heath vegetation on hilltops and giving way to taller woodland communities further down the slope (Beard 1990). The site has gently undulating topography, with 20-30 m change in elevation from valley floor to ridge. Soils change markedly across the landscape, with shallow lateritic duricrusts (coarse sand of 0.1 - 0.2 m depth over laterite) at elevated positions supporting heath vegetation, texture-contrast (coarse sand ~ 0.8 - 1 m depth over gravel/clay) soils further down the slope supporting mixed heath and mallee ('mallee' is the Aboriginal term for shrub-

like multi-stemmed eucalypts) communities, and eucalypt woodlands on the deeper finer-textured (sandy loam of 0.1 m over deep clay) valley floors.

Twenty-one prominent species were selected from across these three contrasting community types (Table 1) to incorporate some of the diversity of leaf types, taxa and growth habits within each community. These three sites represent different positions along the catenary sequence and soil depth, and water-storage capacity increases down the slope. In a related study (Mitchell et al. 2008, *in prep*) leaf areas in five random plots (36 m^2 for heath and mallee sites and 100 m^2 for the woodland site) at each site were measured and the selected species represented between 60 – 95% of the total projected leaf area in each plot. Mean species richness from these plots was 16.2, 6.4 per 36 m^2 for the heath and mallee sites and 3.7 per 100 m^2 for the woodland site. Two common root hemiparasitic species, *Santalum acuminatum* (R. Br.) A. DC. (quandong, a shrub or small tree) and *Nuytsia floribunda* (Labill.) Fenzi (Western Australian Christmas tree), were among the species selected. All species selected are evergreen and retain leaves for at least 2 years (personal observation).

The climate at this site is characterised as dry warm Mediterranean, with a long-term annual rainfall of 375 mm, most of which falls during the winter months of May to August. Mean monthly evaporation ranges from 240 – 280 mm during summer months (December-February) and exceeds precipitation for most months of the year. The annual rainfall during the period over which measurements were taken was 352 mm for 2004 and 361 mm for 2005, and only 37 mm fell between December 2004 and February 2005 compared to the 10-year average of 65 mm for this period (Bureau of Meteorology, 2007).

Traits used in this study were chosen to construct an orthogonal species-trait matrix based on

1) their relevance to the central objective of this study, 2) practicalities in their collection and measurement, 3) their ability to define trade-offs in water use or capture responses to changes in water availability. In total there were 16 traits used in the multivariate analyses.

Leaf water relations and specific leaf area

Leaf water potentials (Ψ_{leaf}) at pre-dawn were used to infer average soil water status across the root-soil interface. Spring-time (September) pre-dawn Ψ_{leaf} (Ψ_{leaf} max) was assumed to be representative of maximum or close to maximum values of leaf water status, and early autumn (March) midday values of Ψ_{leaf} (Ψ_{leaf} min) were assumed to represent minimum values of leaf water status. Seasonal differences in pre-dawn Ψ_{leaf} ($\Delta\Psi_{leaf}$) were also included as a trait to explain shifts in water availability during wet periods (early spring) and dry periods (early autumn). Similarly stomatal conductance (g_s) measured in early spring (September, g_s max) and autumn (March, g_s min) represent estimates of maximum and minimum values of g_s for this study. Ψ_{leaf} were measured on healthy, mature leaves on 3 – 5 individuals of each species using two PMS-1000 pressure chambers (PMS Instrument Corvallis, OR, USA). Pre-dawn measurements were made on clear, cloudless mornings between 3 00 – 6 00 h, depending on season. Leaves or leafy twigs were cut, bagged in plastic and transferred promptly to the pressure chamber for measurement. Stomatal conductance to water vapour (g_s) was measured at mid-morning between 10:00 – 12:00 h as an estimate of daily peak water loss, using the Licor 6400 gas exchange system (Licor Instruments, Lincoln, NE, USA). Chamber CO_2 concentration was set at 360 μmol mol^{-1} and photosynthetic photon flux density (red-blue light source) at 1500 μmol m^{-2} s^{-1}. Measurements were made on two healthy, sun-lit and fully expanded leaves from each of four individuals per species.

Six mature leaves were also collected from each species to measure specific leaf area (*SLA*; $m^2\ kg^{-1}$). Leaves were scanned using a Licor 6100 (Licor Instruments, Lincoln, NE, USA) to determine leaf area. Leaves were then placed in an oven at 70°C for 48 h for determination of dry mass. *SLA* was calculated by dividing the leaf area by the leaf dry mass.

Leaf physiological parameters related to turgor maintenance, namely osmotic potential ($\Psi_{\pi 100}$) and maximum bulk modulus of elasticity (ε_{max}) during spring and summer were taken from related work involving 20 of the 21 species (Mitchell et al. *in prep*). Pressure-volume analyses were performed on leafy twigs in September 2004 and February-March 2005 collected between 4 00 – 7 00 h. Four – five leaf or leafy twig samples per species were rehydrated and transported to the laboratory, and curves were generated using the bench-drying technique (Turner, 1988). Summer pressure-volume analysis of *Actinostrobus arenarius* C. A. Gardner was not possible, due to the difficulty of rehydrating the tissue during summer. The two leaf physiological parameters included in this study represent the seasonal shifts in these traits calculated using the difference in summer and spring values, and denoted by $\Delta\Psi_{\pi 100}$ and $\Delta\varepsilon_{max}$.

Hydraulic conductivity

All stems for hydraulic conductivity measurements were collected in the field between 4 00 and 7 00 h to minimise the effect of diurnal changes in hydraulic conductivity (*K*). Six to eight stems per species were sampled during September 2004 and March 2005. Twig samples were collected on different individuals during each season to minimise the impact of the sampling on the small plants of many of the species. Large leafy branches were cut (distal to the leaves) and bagged in large plastic bags containing moist paper towels, sealed and re-bagged, transported to the laboratory and stored at 4 ºC. At the time of measurement

of *K*, stems were recut under water at a length approximately two times greater than the maximum vessel length (0.2 – 0.8 m), and stem widths varying from 3 -10 mm.

The apparatus for measuring hydraulic conductivity was similar to that described by (Sperry 1988). It comprised a reservoir of 0.01 M KCl filtered, deionised water elevated to a height of ~0.3 m thus creating a head pressure of ~0.003 MPa. Small-diameter (6 mm) polypropylene tubing connected the reservoir to a luer lock valve, and silicon tubing connected the valve to the distal end of the stem segment. The proximal end of the stem segment was connected in a similar fashion and the tubing led to a measuring cylinder resting on an electronic balance (Ohaus, NJ, USA; ±0.001 g resolution). The weight of water flowing through the system was logged on a computer at 10 s intervals. Once the stem segment was attached, water was passed through the segment for 2 – 3 mins until a steady flow rate was graphically observed on the computer. This first measurement represented native flow rate. Stem segments were then flushed for 20 mins (using the same solution and pressure from a captive air tank) at ~ 0.03 MPa for the conifer species and at ~ 0.08 MPa for all other species so as not to damage pit membranes whilst flushing. Low pressure was then reapplied for measurements of flow rate at maximum flow rate. Repeated flushing on each species revealed that 20 mins was sufficient to achieve a maximum flow rate. Flow rates were calculated by a linear regression of weight change versus time on the balance. Reservoir and balance water levels were also recorded to calculate the exact pressure head, and from the above parameters hydraulic conductance (kg s^{-1} MPa^{-1}) and *K* (after multiplication by length of stem segment; kg s^{-1} m MPa^{-1}) were calculated. Stem cross-sectional area at the distal end of the stem was used to calculate stem-specific *K* or K_S (kg m^{-1} s^{-1} MPa^{-1}). The diameter of pith regions in the stem was measured and the total pith area (ranged from 3 – 10 % of total stem cross-sectional area) was subtracted from the total cross-

sectional areas of the stem. Leaf area was also measured on leaves above the proximal end of the stem segments for determination of leaf-specific hydraulic conductivity ($K_{L,}$ kg m^{-1} s^{-1} MPa^{-1}). Huber values (*HV*) were calculated by dividing the distal cross-sectional area by the total branch leaf area.

Percentage embolism for both summer samples was calculated according to:

% embolism = (1 - (native K_S / maximum K_S)) * 100 Equation 1

Conduit Anatomy

All stem samples of the 21 species used in hydraulic conductivity measurements (above) were used for measurement of conduit diameter. Two transverse sections at both ends of these stem sections were made using a hand microtome at 20 – 30 µm thickness. Intact stem sections were then stained with basic fuchsin, rinsed and transferred to slides for microscopy. Digital images of sapwood material were made using a compound light microscope and digital camera at 50 x (Carl Zeiss Inc., NY). All but one species contained diffuse-porous wood, and only the outer radial half of xylem conduits was included for analysis or, in the case of *A. arenarius* (conifer), the most recent growth ring. Diameters of conduits were measured using imaging software (Image J, 1.32J, USA Institutes of National Health), by first creating threshold values from the black and white images and then analysing average diameter for all conduits within the sapwood. Hydraulically weighted mean conduit diameter was calculated on each sapwood segment (n > 100 conduits), and a grand mean was determined for each species to determine the relative contribution of the conduit to hydraulic conductivity. This calculation is based on the Hagen-Poiseuille relationship, whereby a conduit's contribution to the hydraulic conductivity is proportional to the fourth power of its diameter (d). We used $(\sum d^4/n)^{¼}$ to generate the hydraulically weighted mean conduit diameter of each section and species based on this hydraulically weighted distribution. Total

lumen area and conduit density were also calculated on each section by using the sum of the total conduit areas or the conduit count per image divided by the total area of each analysed image.

Water use efficiency

The ratio of CO_2 assimilation and g_s is a measure of intrinsic water use efficiency (*WUE*) and can be assessed using the ratio of the heavier ^{13}C isotope to ^{12}C ($^{13}C/^{12}C$). This is because fractionation of ^{13}C occurs during photosynthetic CO_2 fixation and is linearly related to the concentration of intercellular CO_2 relative to atmospheric CO_2 (C_i/C_a) (Farquhar et al. 1982). The C_i/C_a value differs among co-occurring species because of interspecific variation in photosynthetic capacity and/or g_s. Thus, analysis of $^{13}C/^{12}C$ of leaf material provides a time-integrated measure of intrinsic *WUE* over the period in which the leaf carbon is assimilated.

Three leaves from the same individuals sampled for leaf water potential during January were collected for determination of carbon-isotope composition ($\delta^{13}C$). Leaves from the previous year's cohort were collected to obtain material > 12 months old. Leaves were oven dried and ground before being weighed into tin caps on a five-decimal balance before analysis. Carbon isotope composition was analysed using VG SIRA 9 mass spectrometer (Middlewich, UK) and $\delta^{13}C$ was calculated using:

$$\delta‰ = (R_{sample}/R_{standard} - 1) \times 1000 \quad \text{(Farquhar et al. 1982)} \qquad \text{Equation 2}$$

where R_{sample} and $R_{standard}$ are the abundance ratios, $^{13}C/^{12}C$, of the sample and the standard, Pee Dee Belemnite (Keeling et al. 1979), respectively.

Biomass allocation

Root:stem cross-sectional areas were used as an indicator of allocation strategy between

stems and roots. Root and stem diameters were measured using digital callipers at 0.1 m from the root junction or lignotuber or above the soil surface (for stems) to avoid large increases in root diameters near the root junction. Three to four individuals per species were excavated using a supersonic air spade (Series 2000, Concept Engineering Group Inc, Verona, PA, USA) that consists of a wand and nozzle that funnels high-pressure air (generated by a compressor) onto the soil, removing soil and fine roots (~< 5 mm) around the plant. Root systems were excavated to depths of ~ 0.8 m, although at the heath and woodland sites excavations were often shallower due to the presence of impenetrable, fused laterite or heavy clay.

Sapwood density

Small 2-3-year-old stem material (~ 3-6 mm diameter) was sampled from six individuals per species in December 2004. Stem segments of ~ 40 mm were cut and the periderm removed and immediately transferred to vials in a portable refrigerator to prevent dehydration of samples. We estimated that the pith region in the stem segments used for density measurements represented < 5% of the total stem cross-sectional area. Fresh wood volume (V_f) of these segments was measured using the Archimedes principle. Stem segments were attached to a needle tip supported by a clamp on a retort stand and then lowered into a beaker of water of known mass on a balance (±0.0001 g resolution). Each segment was immersed just below the water surface and V_f measured as weight increase owing to the weight of water displaced by the sample. The stem segment was then air dried in an oven at 70 ºC for a minimum of 4 days and weighed to determine dry weight (W_d). Basic density (D_{stem}) of the stem segment was calculated by dividing W_d by V_f.

Statistical Analysis

Two-way trait correlations among relevant physiological and morphological traits were assessed by testing whether the Pearson's correlation coefficient was significantly different from 0 using a 95 % confidence interval (Instat+ v.3.036, University of Reading, UK).

A species x trait matrix was produced for multivariate analysis using site as a factor. A natural log transformation was performed on Huber values and all traits were normalised. Missing variables were assigned values using an expectation maximum likelihood algorithm, which assumes a multi-normal distribution model for the data. Only two missing values of $\Delta\varepsilon_{max}$ and $\Delta\Psi_{\pi 100}$ were estimated for *A. arenarius*, due to difficulties in rehydrating leaf material in summer. Principal Components Analysis (PCA) was performed using Primer 6.1.5 (Primer-E, Plymouth, UK) on the normalised data as it best preserves distance among the measured variables. Eigen vectors, which are coefficients of the linear combinations of trait variables making up each principal component, were also generated. A one-way SIMPER routine using Euclidean distance was performed on the normalised data to analyse the relative contributions of each trait variable to overall variation within and between sites. A linkage tree analysis was performed using the LINKTREE routine (Primer-E, Plymouth, UK) that creates binary splits of species based on maximising the rank similarity statistic, *R*. At each split the routine provides a measure of the separation between the two groups based on the entire ranked similarity matrix, so that splits further down the y-axis (smaller %B values) have smaller overall differences between groups. To determine discrete HFTs we used a cut off of >50 %B of the overall branch length. The routine also determines which variables or traits are responsible for the greatest dissimilarity between the two groups created in each split.

Results

Similarity within and between sites

Results from the one-way SIMPER routine analysis highlighted the degree of similarity in trait values among and between sites (Table 2). Based on average squared distance values, the heath site had the smallest value (9.15) indicating greater similarity between traits among the 13 heath species sampled (Table 2). This is also supported by the principal components analysis, with a smaller degree of scatter between heath species (Fig. 1a) than for the other sites. Woodland species displayed greatest variation in traits with an average squared distance value of 24.95 (Table 2) and a larger degree of scattering within the first two principal components (Fig. 1a). As expected, between-site variation was larger than within site variation particularly between the woodland site and heath and mallee sites (37.89 and 42.53 respectively; Table 2). Simper routine differences for individual traits (data not shown) indicated $\Delta\Psi_{\pi\,100}$, g_s max and Ψ_{leaf} min were the largest contributors to site variation among heath species (~40% of total trait variation). However, *SLA*, g_s min and K_S were very similar among heath species, representing only ~10 % of the trait variation. In the mallee community differences in *SLA*, stem hydraulic traits (conduit diameter and max % embolism), wood density and Ψ_{leaf} min accounted for over 50 % of the variation. Species differences in the woodland community were due to variation in leaf/stem area allocation (*HV*), hydraulic parameters (K_S and conduit diameter), tissue elasticity ($\Delta\varepsilon_{max}$) and water use efficiency ($\delta^{13}C$), (~45 %).

Trait relationships

The first two principal component axes accounted for 64% of the total variation in trait values. Not surprisingly, the hydraulic traits such as K_S, conduit diameter and max % embolism in summer clustered together and loaded strongly on the first principal component (PC1; Fig. 1b and Table 3). Accordingly, the three *Eucalyptus* species and the root

hemiparasite *S. acuminatum* were located in the same direction, indicating a strong positive effect of these hydraulic traits in determining their position (Figs 1a and b). There was also a clustering of other non stem-specific hydraulic traits including K_S and *HV* with δC^{13} (Fig. 1b, Table 3). Traits such as stem:root cross-sectional areas, g_s min, $\Delta\varepsilon_{max}$ and $\Delta\Psi_{\pi 100}$ appeared to have a very small effect on the overall species positioning as indicated by their shorter eigen vectors (Fig. 1b). $\Delta\Psi_{leaf}$ and Ψ_{leaf} min had longer eigen vectors in opposite directions, representing a negative correlation and contributing a greater influence on the overall species positioning in the first two principal component axes (Fig. 1b). Leaf physiological traits $\Delta\Psi_{\pi 100}$ and $\Delta\varepsilon_{max}$ were positively correlated, (Table 3) and had only a moderate effect on the overall species positioning. *SLA* loaded strongly on PC1 and was negatively correlated $\Delta\Psi_{\pi 100}$ (Fig 1b, Table 3) and $\Delta\Psi_{\pi 100}$ showed a strong positive relationship to Ψ_{leaf} at turgor-loss point (data not shown).

The scatter plots shown in Figure 2 present some of the important relationships between traits among the 21 species. The traits along each of the x-axes: wood density, $\delta^{13}C$ and *SLA*, help to clarify important species relationships and possible key axes of plant strategy with respect to carbon and water balance. Wood density had no relationship to water-transport efficiency (hydraulic conductivity) based on both K_L and K_S (Fig. 2a and b). A negative correlation exists between Ψ_{leaf} min and wood density (r = 0.65 $P<0.05$, Fig 2c). Additional regression analyses using both total lumen area and conduit density as explanatory variables showed a significant negative relationship between wood density and total lumen fraction (r = 0.65, $P<0.05$) and no relationship to conduit density among the 20 angiosperm species. Alternatively, K_S was negatively associated with conduit density (r^2 = 0.90, $P<0.01$) and showed no relationship to total lumen area. *SLA* was negatively correlated to $\Delta\Psi_{leaf}$ (r^2 = 0.59, $P<0.05$) (Fig. 2d) and positively correlated to g_s max (r = 0.44, $P<0.05$) (Fig 2e),

particularly in heath species. *SLA* showed a positive correlation to conduit diameter (r = 0.51, $P<0.05$, Fig. 2f), a trait tightly linked to K_L and max % embolism (Table 3 and Fig. 1b). Leaf $\delta^{13}C$ values correlated positively to $\Delta\Psi_{leaf}$ (r = 0.48, $P<0.05$, Fig 2g) and negatively with minimum Ψ_{leaf} (r = 0.48, $P<0.01$, Fig. 2h), but showed no relationship to either g_s min or g_s max (Fig. 2i).

Species groupings

The LINKTREE graph shows the hierarchy of branching points among the 21 species, and five groupings of HFT's were classified based on their water use strategy. These ranged from year-round active tree and shrub, hemiparasite and drought-suppressed broad-leaved and narrow-leaved shrub HFTs (Fig. 3). The initial branching point in the LINKTREE (split i) splits the year-round active tree and shrub HFT from the drought-suppressed shrub and parasite HFTs (Fig 3). The year-round active tree and shrub HFTs diverges strongly from the remaining HFTs, largely due to the maintenance of higher g_s during summer (Fig 3). Split ii separates the year-round active shrub *Grevillea patentiloba*, from the tree groups due to reduced hydraulic transport efficiency (K_S, conduit diameter) (Fig. 3). Split iii separates the remaining species (two drought-suppressed shrub types and hemiparasite) and was due largely to differences in values of Ψ_{leaf} min (Fig 3) and in leaf physiology and structure. The fourth split separating the hemiparasite HFT from drought-suppressed broad-leaved shrub HFT was due mostly to reduced wood density in the hemiparaste and to greater % embolism in summer and vessel diameter. (Fig. 3). The drought-suppressed broad-leaved shrub HFT tended to have greater $\delta^{13}C$ values, less negative Ψ_{leaf} min, larger $\Delta\Psi_{\pi 100}$ and higher *SLA* (Fig 1a and b). The drought-suppressed narrow-leaved shrub HFT tended to have lower $\delta^{13}C$ values, less osmotic adjustment between spring and summer ($\Delta\Psi_{\pi 100}$) and lower *SLA* (Fig 1a and b). However, species within both of these drought-suppressed shrub HFTs had similar g_s

values during summer, reduced hydraulic efficiency and a large allocation of root biomass, with the exception of the understorey shrub, *Olearia axillaris*.

Discussion

Trait variation and water use patterns along the gradient

The variability in traits at different sites reflects differences in community structure and adaptations to different water-availability regimes and soils. Thus the water use strategies observed in this study tend to lie along a continuum ranging from year-round active species that have a more buffered response to summer water deficit whereas the drought-suppressed species exhibit significant declines in their water use capacity (Fig 3). The apparent convergence in trait values at the heath site, a site characterised by shallow soil and reduced water availability, suggests that strategies exhibited by most species in this habitat are strongly constrained by the low soil water potentials and limited rooting volumes. These xeric conditions favour increased hydraulic safety at the expense of hydraulic efficiency, more allocation toward root biomass and thicker/denser leaves (lower *SLA*). The availability of water is highly seasonal at this site with average $\Delta\Psi_{leaf}$ values of -3.7 MPa, and differences in the two dominant HFTs, the drought-suppressed narrow- and broad-leaved shrubs are based on variation in leaf physiology ($\Delta\Psi_{\pi 100}$ and $\Delta\varepsilon_{max}$) and levels of carbon-isotope fractionation. Not surprisingly, the root hemiparasite *Santalum acuminatum*, was able to overcome these limitations by parasitising its surrounding hosts, and exhibited a water use strategy that more closely resembles the tree species, and hence it was grouped to the year round-active tree HFT.

At the other end of the water-availability gradient, the woodland community had the greatest overall variability in trait values (Table 2). The taller stature of plants at this more mesic site

permits stratification of the plant canopy with concomitant changes to light- and water-harvesting strategies by plants. Consequently, three quite different HFTs were found at the woodland site (Fig 3). Water acquisition at this site appears to be partitioned between year round-active shrub and tree HFTs and the drought-suppressed shrub HFT. Niche overlap with respect to water resources is reduced among these woodland species by virtue of the deeper soil. Importantly, these deep soils reduce the need for greater below-ground investment (increased stem:root values), support greater leaf area and steady carbon fixation, all of which allow plants of considerable above-ground stature (i.e. trees of 15-25 m) to establish. Beneath these large plants, understorey species comprising differing HFTs can establish. The year round-active shrub *G. patentiloba* maintained high g_s min and small seasonal fluctuations in pre-dawn Ψ_{leaf} (-1.2 MPa) in keeping with access to deep soil water via its large taproot (*personal observation*), yet on the other hand retains conservative characteristics like reduced *SLA* and reduced hydraulic efficiency (although some of these characteristics may reflect constraints other than water). The deep-rooting habit of *G. patentiloba* reduces competition for soil water with other shallower-rooted understorey species. The shallow-rooted *O. axillaris* experienced large seasonal reductions in pre-dawn Ψ_{leaf} (-5.2 MPa) and is equipped with many of the attributes common to the heath species; it has been grouped in the drought-suppressed narrow-leaved HFT.

Trade-offs in water transport and safety

The hydraulic safety/efficiency trade-off proposed by Zimmerman (1983) and Tyree, (1994) was evident among the 21 species we investigated from strong correlations between conduit diameter, K_S and max % embolism (Fig. 1b). However, wood density, which has previously been found to be an important correlate of hydraulic efficiency (Meinzer 2003; Wagner 1998) was not significantly correlated with K_S or K_L (Fig. 2a) or the other hydraulic traits (Fig. 1b).

The lack of such a relationship between these traits comes about because wood density largely reflects lumen area, since the density of woody matter itself is relatively invariant (Siau 1971). Wood density may have little bearing on hydraulic efficiency, since the same lumen area can be divided up into many small (inefficient) conduits or fewer large conduits whose conductivity increases with the 4^{th} power of their diameter. Additional analyses of conduit configuration among the 21 species support the concept that conduit characteristics can vary significantly within a narrow range of wood densities (Searson et al. 2004), leading to large differences in transport efficiencies. Lumen fraction largely determined wood density in the study species, a result consistent with other species in Mediterranean-type ecosystems (Preston and Ackerly 2003) and reflects carbon-allocation strategy within sapwood, yet does not predict the water-transport efficiency through sapwood. These results are supported by Roderick (2001) who used a pipe model to test the sensitivity of flow rate to changes in wood density, and found that flow rate was only sensitive to variation in density in gymnosperm species, due to the relatively small variation in tracheid diameters.

Wood density did correlate negatively to minimum Ψ_{leaf} (Fig. 2), a trait that is strongly linked to soil water availability, stomatal response and the hydraulic architecture of many species from a range of different environments (Bhaskar and Ackerly 2006). Because plants often transport water at tensions close to cavitation thresholds in order to maintain water uptake in drying soils (Sperry et al. 2002), Ψ_{leaf} min is likely to reflect a minimum operating tension at which 'catastrophic' cavitation is avoided and physiological activity is maintained. The relationships observed in this study between wood density, Ψ_{leaf} min and hydraulic efficiency traits suggests that different species may have similar wood densities (and lumen fraction within the sapwood) and experience similar minimum xylem tensions in the dry period, yet have very different conduit anatomies and hydraulic efficiencies. It is likely that a variety of

other anatomical factors such as the reinforcement of pit structures to reduce the risk of air-seeding (Sperry and Hacke 2004; Burgess et al. 2006); improve species tolerance to low Ψ_{leaf} min and permit the observed variation in hydraulic efficiency (via larger conduit diameters and reduced conduit densities) in species with similar wood densities.

Water use efficiency and water spending

$\delta^{13}C$ values indicated greater fractionation of ^{13}C in species that had less access to water in summer and greater seasonal shifts in water availability (more negative Ψ_{leaf} min, Fig. 2g, 2h) and suggest that these species exhibited less stomatal closure during periods in which leaf carbon was assimilated. The growth period in these species (predominantly from the heath site), is generally in early spring (Pate et al. 1984; Veneklaas and Poot 2003) when pre-dawn Ψ_{leaf} values are quite high (Fig. 4a), indicating good access to water, and such conditions may promote less stomatal limitation to CO_2 diffusion. Conversely, tree species that exhibited less fractionation and less negative summer Ψ_{leaf} initiate growth in early summer, a period during which greater stomatal limitation will occur due to strongly increasing evaporative demand and declining soil water potential. The less-conservative strategy in terms of stomatal control observed in the present shallow-rooted drought-suppressed species has also been observed in grassland communities where species that are physiologically active in the early, less stressful months of the growing season showed more discrimination against ^{13}C (Smedley 1991).

The $\delta^{13}C$ values reported here represent intrinsic *WUE* (A/g_s), but may not adequately reflect long-term integrated carbon gain (A) per unit of water lost in transpiration (E) among the 21 different species, because transpiration not only depends on g_s, but also on the vapour pressure deficit (*VPD*), which differs among seasons. Such variation in *VPD* during growth

periods when most carbon assimilation occurs would alter levels of water loss in leaves for a given value of g_s. Species comparisons of $\delta^{13}C$ values are also affected by the variation in mesophyll resistances for CO_2 diffusion that may change in response to *VPD* (Bongi and Loreto 1989), leaf age (Niinemets et al. 2005), temperature (Bernacchi et al. 2002) and a host of other external and internal factors (Flexas et al. 2007). Therefore, we exercise some caution when interpreting $\delta^{13}C$ values to assess whole plant relationships in carbon gain per unit water lost without a full appraisal of seasonal responses to water availability and *VPD* and interspecific and temporal variation in mesophyll resistances.

Leaf structure and water supply

SLA was negatively correlated with seasonal changes in water status ($\Delta\Psi_{leaf}$), hydraulic efficiency (conduit diameter), and maximum g_s during spring (Figs 2d-f). *SLA* is a key trait that reflects the investment of leaf mass for a given light-harvesting potential, and is strongly associated with photosynthetic capacity (Field and Mooney 1986; Reich et al. 1998), leaf life span (Westoby et al. 2002; Wright et al. 2004) and adaptations to water stress (Niinemets 2001). At the woodland site where more favourable soil water availability produces a taller, stratified canopy there is a larger divergence in *SLA* values, reflecting the greater diversity of HFT's. Consistent with the hypothesis of Wright et al. (2002) that SLA converges in drier climates, we observed a greater convergence of low *SLA* values at the sites that were more xeric, not due to climate but to soil water availability. The SLA-g_s max relationship we observed may not represent a mechanistic relationship, but may arise due to selection pressures that maintain associations of both traits to other leaf photosynthetic traits such as maximum rates of photosynthesis and leaf nitrogen concentration. For example, lower-*SLA* species tend to have lower leaf turnover rates and longer return periods per unit of carbon investment, and such a strategy would promote more conservative g_s max in order to maintain

leaf integrity and water balance. These thicker/denser leaves are also able to withstand large seasonal shifts in Ψ_{leaf} that occur at the drier sites and display more negative turgor-loss points, a trait that is influenced by both osmotic and elastic properties of leaf tissue (Mitchell et al. *in prep*).

The HFT approach and key axes of water use strategy

The opposing trends between total species diversity and levels of trait variation across the three sites highlights the value of using HFTs to deconstruct the water use functioning of native vegetation assemblages. Niche differentiation regarding water use does not appear to contribute to the greater species diversity along this gradient, suggesting other factors such as nutrition and disturbance (e.g. fire) need to be invoked to explain these local patterns of biodiversity (Hopper and Gioia 2004). Interestingly, there was a fair degree of trait similarities among species at the genus level (Fig. 3) which suggests that many of these water use traits represent earlier adaptations to water limitation and have been retained among different species of the same genus.

In this study, *SLA* and Ψ_{leaf} min were useful predictors of likely water use strategies and the distribution of species within HFTs that range from year round-active trees to drought-suppressed shrubs is strongly constrained by these two traits (Table 3). Although these two traits were positively correlated ($P<0.05$), they tended to be associated with different suites of traits with *SLA* and Ψ_{leaf} min loading more strongly on PCA 1 and PCA 2 respectively (Fig. 1 and 2). In this ecosystem where competition for light is of limited relevance, *SLA* integrates both carbon and water use capacity along the water-availability gradient. This study suggests that *SLA*, in addition to well established trade-offs concerning the leaf economic spectrum (Wright et al. 2004), is also associated with water-transport efficiency, high g_s and leaf turgor

maintenance. Ψ_{leaf} min represents potential tolerance limits of seasonal water deficit and is affected by soil texture (Sperry and Hacke 2002), depth, availability of water at the root surface and shifts in the daily transpirational demand. Thus, the tolerance of large negative tensions during summer was associated with denser wood (Fig 2c). The importance of both traits is evident in similar ecosystems, such as the California chaparral communities (Ackerly 2004) and is likely to define water use strategies across many vegetation types.

Conclusions

In conclusion, we suggest the HFT approach not only elucidated the key dimensions of water use strategies in the ecosystem under investigation, but it is also a successful tool for characterising the water use functioning of species-rich vegetation assemblages. The predominance of combinations of different HFTs provide important clues as to the degree of water use partitioning that is possible under differing soil types; information that is vital in southern Australia where there is a need for revegetation methods that maximise the capture of rainfall along soil gradients. For example the convergence of trait values and dominance of the drought-suppressed shrub HFTs at the heath site, suggest only species exhibiting a limited set of suitable traits will be viable in shallow, ridge-top sites. A greater variety of trait combinations are possible for revegetation of mid and bottom slope sites so that the introduction of complementary HFTs at these sites will promote greater water use partitioning and increase total water use capacity. The five HFTs are likely to be broadly applicable to other biomes particularly where water availability is strongly seasonal (although the hemiparasite HFT will be less common), but we expect some plasticity in their groupings along a continuum of water use responses.

Acknowledgements

The authors acknowledge the assistance in the laboratory and field of Perry Swanborough, Catarina Mata, Pachi Baquedano and Robyn Campbell. Financial support of this project was from the Cooperative Research Centre for Plant-Based Management of Dryland Salinity and permission to work at the Corrigin Water Reserve was granted by the Water Corporation of Western Australia.

References

Ackerly D (2004) Functional strategies of chaparral shrubs in relation to seasonal water deficit and disturbance. Ecol Monogr 74 25-44

Beard JS (1980) The vegetation of the Corrigin area, Western Australia. Veg Map Publications, Perth

Beard JS (1990) Plant Life in Western Australia Kangaroo Press, Sydney

Bernacchi CJ, Portis AR, Nakano H, von Caemmerer S, Long SP (2002) Temperature Response of Mesophyll Conductance. Implications for the Determination of Rubisco Enzyme Kinetics and for Limitations to Photosynthesis in Vivo. Plant Phys130 1992-1998.

Bongi G, Loreto F (1989) Gas-exchange properties of saltstressed olive (*Olea europaea* L.) leaves. Plant Phys 90 1408-1416.

Bureau of Meteorology (2007) Climate Averages for Corrigin. Australian Government, Canberra ACT [updated 2006; cited 15 July 2007]. Available from http://www.bom.gov.au/climate/averages/tables/cw_010536.shtml.

Burgess SSO, Pittermann J, Dawson TE (2006) Hydraulic efficiency and safety of branch xylem increases with height in Sequoia sempervirens (D. Don) crowns. Plant Cell Environ 29 229-239

Bhaskar R, Ackerly DD (2006) Ecological relevance of minimum seasonal water potentials. Physiol Plantarum 127 353-359

Dirnböck T, Hobbs RJ, Lambeck RJ, Caccetta PA (2002) Vegetation distribution in relation to topographically driven processes in southwestern Australia. Appl Veg Sci 5 147-158

Eagleson PS (1982) Ecological optimality in water-limited natural soil-vegetation systems 1. Water Resour Res 18 325-340

Enquist BJ (2003) Cope's Rule and the evolution of long-distance transport in vascular plants: allometric scaling, biomass partitioning and optimization. Plant Cell Environ 26 151-161

Enquist BJ, Niklas KJ (2001) Invariant scaling relations across tree-dominated communities. Nature 410 655-660

Farquhar GD, O'Leary MH, Berry JA (1982) On the relationship between carbon isotope discrimination and the intercellular carbon dioxide concentration in leaves. Aust J Plant Phys 9 121-137

Field C, Mooney HA (1986) The photosynthesis-nitrogen relationship in wild plants T J Givnish(eds) In: On the Economy of Plant Form and Function. Cambridge University Press, pp 25-55

Flexas J, Ribas-Carbo M, Diaz-Espejo A, Galmès J, Medrano H (2007) Mesophyll conductance to CO2: current knowledge and future prospects. Plant Cell Environ 31 602-621

Hacke UG, Sperry JS, Pockman WT, Davis SD, McCulloh KA (2001) Trends in wood density and structure are linked to prevention of xylem implosion by negative pressure. Oecologia 126 457-461

Hatton TJ, Nulsen RA (1999) Towards achieving functional ecosystem mimicry with respect to water cycling in southern Australian agriculture. Agroforest Syst 45 203-214

Hatton TJ, Salvucci GD, Wu HI (1997) Eagleson's optimality theory of an ecohydrological equilibrium: quo vadis? Funct Ecol 11 665-674

Hopper SD, Gioia P (2004) The southwest Australian floristic region: evolution and conservation of a global hot spot of biodiversity. Annu Rev Ecol Evol S 35 623-650

Keddy PA (1992) Assembly and response rules: two goals for predictive community ecology. J Veg Sci 3 157-164

Keeling CD, Mook WG, Tans PP (1979) Recent trends in the 13C/12C ratio of atmospheric carbon dioxide. Nature 277 121-123

Meentemeyer RK, Moody A (2002) Distribution of plant life history types in California chaparral: the role of topographically-determined drought severity. J Veg Sci 13 67-78

Meinzer F (2003) Functional Convergence in plant responses to the environment. Oecologia 134 1-11

Meinzer FC, Goldstein G, Andrade JL (2001) Regulation of water flux through tropical forest canopy trees: do universal rules apply? Tree Phys 21 19-26

Niinemets U (2001) Globa-scale climatic controls of leaf dry mass per area, density and thickness in trees and shrubs. Ecology 82 453-469

Niinemets U, Cescatti A, Rodeghiero M, Tosens T (2005) Leaf internal diffusion conductance limits photosynthesis more strongly in older leaves of Mediterranean evergreen broad-leaved species. Plant Cell Environ 28 1552-1566

Pate JS, Dixon KW, Orshan G (1984) Growth form and life form characteristics of Kwongan species J S Pate & J S Beard (eds) In: Kwongan Plant Life of the sandplain. University of Western Australia, Perth,

Peck AJ, Hatton TJ (2003) Salinity and the discharge of salts from catchments in Australia. J Hydrol 272 191-202

Preston KA, Ackerly DD (2003) Hydraulic architecture and the evolution of shoot allometry in contrasting climates. Am J Bot 90 1502-1512

Reich PB, Ellsworth DS and Walters MB (1998) Leaf structure (specific leaf area) modulates photosynthesis–nitrogen relations: evidence from within and across species and functional. Funct Ecol 12 948-958

Reich PB, Walters MB and Ellsworth D S (1997) From tropics to tundra: global convergence in plant functioning. Proceedings of the National Academy of Sciences USA 94 13730-13734

Roderick ML, Berry SL (2001) Linking wood density with tree growth and environment: a theoretical analysis based on the motion of water. New Phytol 149 473-485

Searson MJ, Thomas DS, Montagu KD, Conroy JP (2004) Wood density and anatomy of water-limited eucalypts. Tree Phys 24 1295-1302

Siau JF (1971) Flow in Wood Syracuse University Press, London

Smedley MP, Dawson TE, Comstock JP, Donovan LA, Sherrill DE, Cook CS, Ehleringer JR (1991) Seasonal carbon isotope discrimination in a grassland community. Oecologia 85 314-320

Sperry JS, Donnelly JR, Tyree MT (1988) A method for measuring hydraulic conductivity and embolism in xylem. Plant Cell Environ 11 35-40

Sperry JS, Hacke UG (2002) Desert shrub water relations with respect to soil characteristics and plant functional type. Funct Ecol 16 367-378

Sperry JS, Hacke UG, Oren R, Comstock JP (2002) Water deficits and hydraulic limits to leaf water supply. Plant Cell Envrion 25 251-263

Turner NC (1988) Measurement of plant water status by the pressure chamber technique. Irrigation Sci 9 289-308

Tyree MT, Davis SD, Cochard H (1994) Biophysical perspectives of xylem evolution—is there a tradeoff of hydraulic efficiency for vulnerability to dysfunction. International Association of Wood Anatomists Journal 15 335-360

Veneklaas EJ, Poot P (2003) Seasonal patterns in water use and leaf turnover of different plant functional types in a species-rich woodland, south-west Australia. Plant Soil 257 295-304

Wagner KR, Ewers FW, Davis SD (1998) Tradeoffs between hydraulic efficiency and mechanical strength in the stems of four co-occurring species of chaparral shrubs. Oecologia 117 53-62

Westoby M, Falster DS, Moles AT, Vesk PA, Wright IJ (2002) Plant Ecological Strategies: Some Leading Dimensions of Variation Between Species. Annu Rev Ecol Syst 33 125-159

Woodward FI, Kelly CK (1997) Plant functional types: towards a definition by environmental constraints T M Smith, H H Shugart, & F I Woodward (eds) In: Plant functional types: their relevance to ecosystem properties and global change. Cambridge University Press, Cambridge, pp 47-55

Wright IJ, Reich PB, Westoby M, Ackerly DD, Baruch B, Bongers F, Cavender-Bares J, Chapin T, Cornelissen JHC, Diemer M, Flexas J, Garnier E, Groom PK, Gulias J, Hikosaka K, Lamont BB, Lee T, Lee W, Lusk C, Midgley JJ, Navas M, Niinemets U, Oleksyn J, Osada N, Poorter H, Poot P, Prior L, Pyankov VI, Roumet C, Thomas SC, Tjoelker MG, Veneklaas EJ, Villar R (2004) The worldwide leaf economics spectrum. Nature 428 821-827

Wright IJ, Westoby M, Reich PB (2002) Convergence towards higher leaf mass per area in dry nutrient-poor habitats has different consequences for leaf life span. J Ecol 90 534-543

Zimmerman MH (1983) Xylem Structure and the Ascent of Sap Springer Verlag, New York

Figures and Tables

Figure 1. First two axis of a Principal Component Analysis of all 21 species. PC1 represents 51% and PC2 represents 29% of the total variation. (a) Species positionings within the multivariate space, with species (abbreviated using genus and species) grouped into hydraulic functional groups from the LINKTREE analysis and are shown by ovals and circles. Site groupings are represented by (●) woodland, (■) mallee and (▲) heath. (b) Correlation coefficients for all variables represented by eigen vectors (solid arrows).

Figure 2. Scatter plots of selected traits in relation to wood density (g m^{-3}), long-term integrated water use efficiency ($\delta^{13}C$, ‰) and specific leaf area (*SLA*, m^2 kg^{-1}) in 21 species. Lines indicate significant values of Pearson's correlation coefficients using $P<0.05$. a) Wood density vs. maximum stem-specific hydraulic conductivity (K_{max} , kg m^{-2} s^{-1} MPa^{-1})), b) density vs. maximum leaf-specific hydraulic conductivity (K_{leaf}, kg m^{-2} s^{-1} MPa^{-1}) and c) density vs. minimum leaf water potential (Ψ_{leaf} min, MPa). d) *SLA* vs. seasonal change in pre-dawn leaf water potential ($\Delta\Psi_{leaf}$, MPa), e) *SLA* vs. maximum stomatal conductance (g_s max, mmol m^2 s^{-1}) and f) *SLA* vs. hydraulically weighted conduit diameter (µm). g) $\delta^{13}C$ vs. Huber value (ln *HV*, m^2 m^{-2}), $\delta^{13}C$ vs. Ψ_{leaf} min and i) $\delta^{13}C$ vs. maximum (solid squares) and minimum (no fill) stomatal conductance (g_s , mmol m^{-2} s^{-1}).

Figure 3. LINKTREE analysis of all 21 species based on the 16 plant traits. Five hydraulic functional types (HFTs) are assigned based on the grouping of species at %B value of approximately >50 %. The traits that are responsible for each split in the tree are shown and the direction of variation for that trait is shown by plus and minus signs. The *R* statistic, which is a measure of the degree of separation in the two groups, is given at each split along the tree. Site groupings are represented by (●) woodland, (■) mallee and (▲) heath. A water

use strategy axes (dashed line) has been added to the base of the figure to highlight the likely positioning of species along a continuum ranging from year-round active HFTs to drought-suppressed HFTs.

Table 1. List of the 21 species sampled in this study (grouped by site), taxonomic family, habit, specific leaf area (*SLA*, m^2 kg^{-1}, n=6) and height (<1, 1-3 and >3 m intervals). Woodland site: open, eucalypt-dominated overstorey with shrub understorey, comprising *Grevillea patentiloba, Olearia axillaris* and other species. Mallee site: scattered *Eucalyptus albida* (small multi-stemmed tree) and *Nuytsia floribunda* (root hemiparasite) with shrub understorey. Heath site: dense shrub layer dominated by members of Proteaceae, Myrtaceae and Casuarinaceae, and the root hemiparasite *Santalum acuminatum*.

Species	**Family**	**Habit**	***SLA*** **(m^2 kg^{-1})**	**± s.e.**	**Height (m)**
Woodland site					
Eucalyptus capillosa subsp. *capillosa* Brooker &	Myrtaceae	Tree	3.19	0.09	>3
Eucalyptus salmonophloia F.Muell.	Myrtaceae	Tree	3.36	0.19	>3
Grevillea patentiloba F.Muell.	Proteaceae	Shrub	1.24	0.08	<1
Olearia axillaris (DC.) Benth.	Asteraceae	Shrub	1.52	0.52	<1
Mallee Site					
Actinostrobus arenarius C. A. Gardner	Cupressaceae	Tall shrub	1.78	0.07	1 – 3
Eucalyptus albida Maiden & Blakely	Myrtaceae	Mallee	4.29	0.06	>3
Dryandra sessilis (Knight) Domin var. *sessilis*	Proteaceae	Tall shrub	3.20	0.11	1 – 3
Nuytsia floribunda (Labill.) Fenzi	Loranthaceae	Tree/root hemiparasite	2.21	0.09	>3
Heath site					
Allocasuarina campestris (Diels) L.A.S. Johnson	Casuarinaceae	Tall shrub	1.66	0.08	1 – 3
Casuarina humilis (Otto & F. Dietr.) L.A.S. Johnson	Casuarinaceae	Shrub	1.36	0.10	<1
Dryandra vestita Meisn.	Proteaceae	Shrub	2.59	0.08	1 - 3
Dryandra cirsioides A.S. George	Proteaceae	Shrub	2.47	0.08	1 - 3
Isopogon gardneri D. Foreman	Proteaceae	Shrub	1.53	0.12	1 - 3
Isopogon axillaris R.Br.	Proteaceae	Shrub	1.37	0.10	<1
Beaufortia micrantha Schauer var. *puberula* Benth.	Myrtaceae	Shrub	1.72	0.14	<1
Melaleuca scabra R.Br.	Myrtaceae	Shrub	1.93	0.39	<1
Petrophile glauca Foreman	Proteaceae	Shrub	0.98	0.22	1 - 3
Hakea subsulcata Meisn.	Proteaceae	Tall shrub	1.36	0.04	1 - 3
Banksia sphaerocarpa R.Br. var. *sphaerocarpa*	Proteaceae	Shrub	2.66	0.14	<1
Hakea cygna Lamont	Proteaceae	Shrub	2.06	0.04	<1
Santalum acuminatum (R.Br.) A.DC.	Santalaceae	Tree/root hemiparasite	1.62	0.15	1 - 3

Table 2. Average distances (based on Euclidean distance measures) within and between sites using one-way SIMPER routine.

	Heath	**Mallee**	**Woodland**
Within-site variation	9.15	16.41	24.95
	Heath x Mallee	**Heath x Woodland**	**Woodland x Mallee**
Between-site variation	25.11	37.89	42.53

Table 3. Pearson's correlation coefficients for all pairwise trait comparisons.

	Ψ_{leaf} min	$\Delta\Psi_{leaf}$	Ψ_{leaf} max	g_s min	g_s max	$\Delta\Psi_{\pi\ 100}$	$\Delta\varepsilon_{max}$	K_L	conduit diam	max % embolism	*HV*	K_S	density	*SLA*	$\delta^{13}C$
Ψ_{leaf} min															
$\Delta\Psi_{leaf}$	**-0.7113**														
Ψ_{leaf} max	-0.0502	**0.6462**													
g_s min	0.0338	**-0.5536**	**-0.8035**												
g_s max	0.0654	-0.1976	-0.2844	0.2932											
$\Delta\Psi_{\pi\ 100}$	-0.2742	0.2239	0.0477	0.0523	0.0254										
$\Delta\varepsilon_{max}$	-0.4358	0.3695	0.0251	-0.0988	-0.0898	**0.5185**									
K_L	0.0908	-0.1354	0.1513	0.1680	-0.2519	0.1800	-0.2269								
conduit diam.	0.2133	**-0.5733**	**-0.6351**	**0.4162**	**0.3293**	-0.0555	0.0596	-0.2782							
max %	0.1269	**-0.5262**	**-0.6399**	**0.3916**	0.2930	-0.3410	0.0033	-0.2388	**0.8627**						
HV	0.2762	-0.2772	0.0692	0.1386	-0.2493	0.0562	-0.1485	**0.8054**	-0.1185	-0.1580					
K_S	-0.0333	**-0.4164**	**-0.6902**	**0.4738**	**0.4136**	-0.3349	-0.0426	-0.3445	**0.7317**	**0.8223**	-0.4165				
density	**-0.6490**	**0.4761**	0.1006	0.0756	-0.3304	-0.0425	0.2265	0.0029	-0.1381	-0.0729	-0.1241	0.0274			
SLA	**0.5894**	**-0.5939**	**-0.5810**	0.1871	**0.4445**	-0.3571	-0.1880	-0.1302	**0.5126**	**0.4634**	-0.0765	**0.5050**	-0.3180		
$\delta^{13}C$	**0.4753**	**-0.4836**	0.0829	0.1793	-0.0379	-0.0317	-0.3040	**0.5199**	-0.1903	-0.2969	0.3842	-0.2096	-0.1425	0.2990	
stem:root	**-0.3980**	0.2054	-0.1049	0.2499	**0.4521**	0.3229	0.0517	-0.1119	-0.1461	-0.2510	-0.1392	-0.0543	0.1242	-0.1561	-0.1429

Significant result for coefficients are shown in bold for *P*<0.05.

Figures

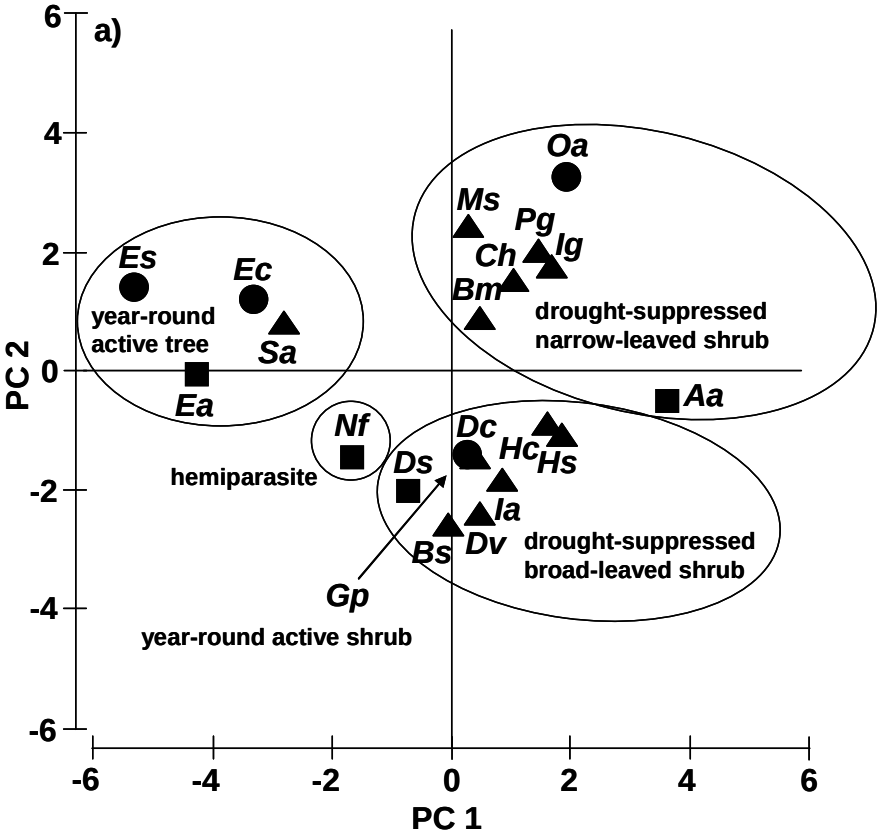
a)
Oa
Ms
Pg
Ig
Ch
Bm
drought-suppressed
narrow-leaved shrub
Es
Ec
Sa
year-round
active tree
Ea
Aa
Nf
hemiparasite
Dc
Hc
Hs
Ds
Ia
Bs
Dv
drought-suppressed
broad-leaved shrub
Gp
year-round active shrub
PC 2
PC 1
6
4
2
0
-2
-4
-6

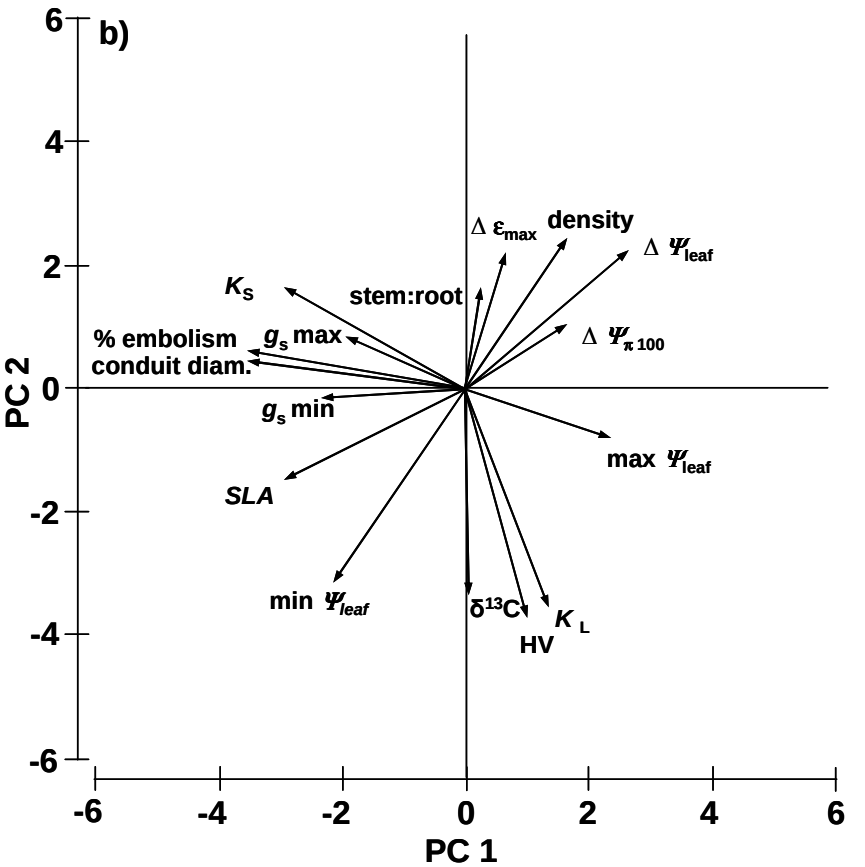
b)
Δ εmax
density
Δ Ψleaf
KS
stem:root
% embolism
conduit diam.
gs max
Δ Ψπ 100
gs min
max Ψleaf
SLA
min Ψleaf
δ13C
KL
HV
PC 2
PC 1
6
4
2
0
-2
-4
-6

Figure 1

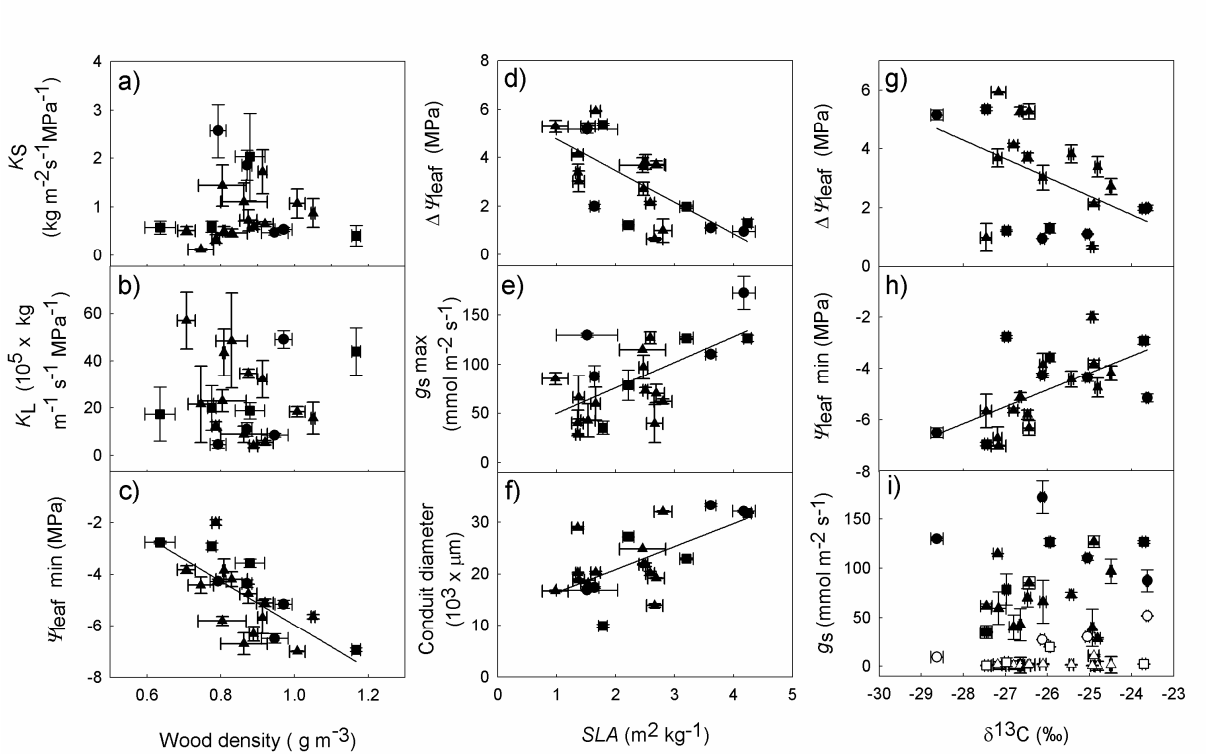

Figure 2

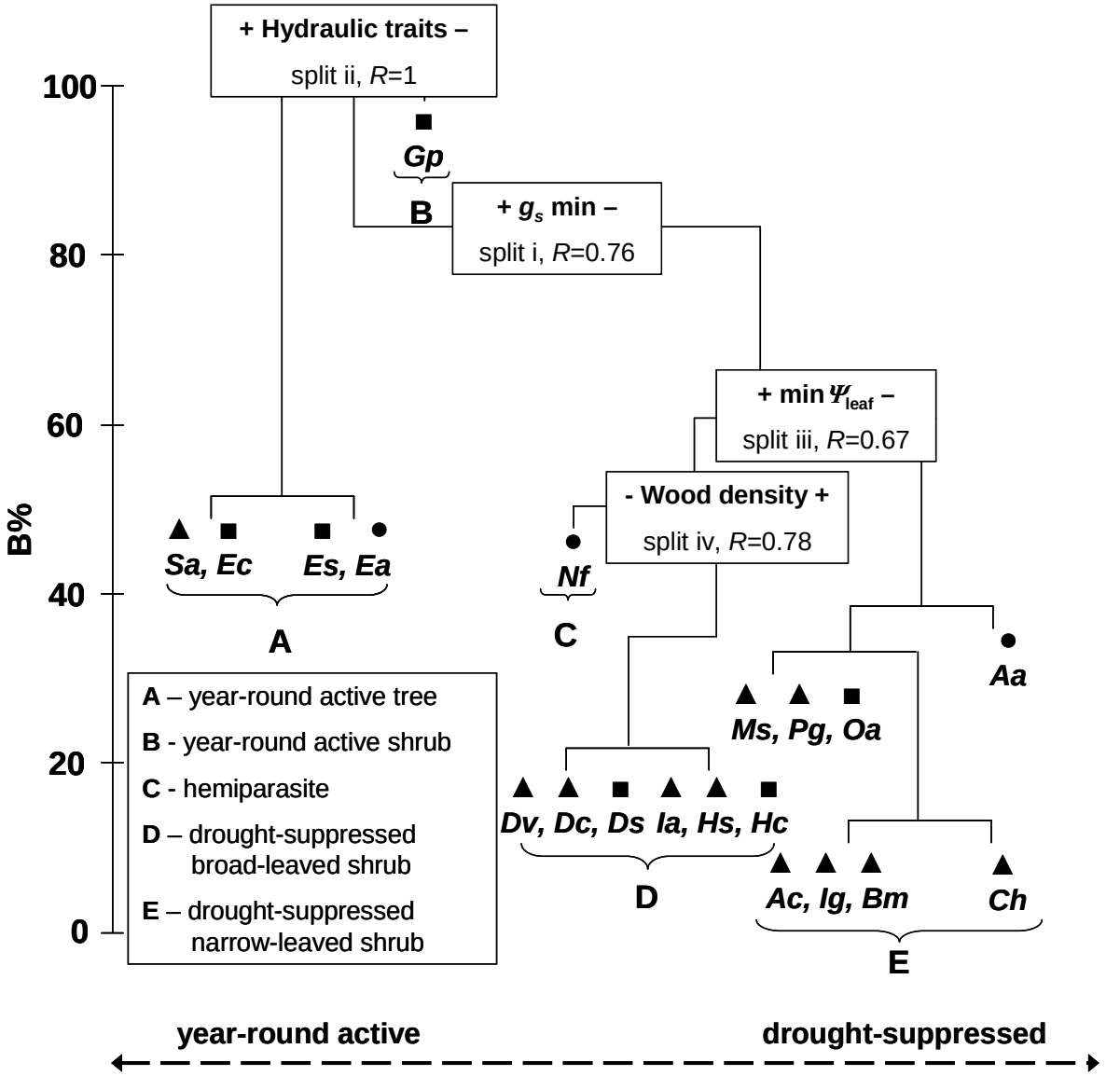
+ Hydraulic traits –
split ii, R=1
Gp
B
+ gs min –
split i, R=0.76
+ min Ψleaf –
split iii, R=0.67
- Wood density +
split iv, R=0.78
Sa, Ec
Es, Ea
A
Nf
C
Aa
Ms, Pg, Oa
Dv, Dc, Ds Ia, Hs, Hc
D
Ac, Ig, Bm
Ch
E
B%
100
80
60
40
20
0
A – year-round active tree
B - year-round active shrub
C - hemiparasite
D – drought-suppressed broad-leaved shrub
E – drought-suppressed narrow-leaved shrub
year-round active
drought-suppressed

Figure 3